

## A comparison of propagated action potentials from tropical and temperate squid axons: different durations and conduction velocities correlate with ionic conductance levels

Joshua J. C. Rosenthal and Francisco Bezanilla\*

Departments of Physiology and Anesthesiology, UCLA School of Medicine, Los Angeles, CA 90095, USA

\*Author for correspondence (e-mail: fbezanil@ucla.edu)

Accepted 5 April 2002

### Summary

To determine which physiological properties contribute to temperature adaptation in the squid giant axon, action potentials were recorded from four species of squid whose habitats span a temperature range of 20 °C. The environments of these species can be ranked from coldest to warmest as follows: *Loligo opalescens* > *Loligo pealei* > *Loligo plei* > *Sepioteuthis sepioidea*. Action potential conduction velocities and rise times, recorded at many temperatures, were equivalent for all *Loligo* species, but significantly slower in *S. sepioidea*. By contrast, the action potential's fall time differed among species and correlated well with the thermal environment of the species ('warmer' species had slower decay times). The biophysical underpinnings of these differences were examined in voltage-clamped axons. Surprisingly, no differences were found

between the activation kinetics or voltage-dependence of Na<sup>+</sup> and K<sup>+</sup> currents. Conductance levels, however, did vary. Maximum Na<sup>+</sup> conductance ( $g_{Na}$ ) in *S. sepioidea* was significantly less than in the *Loligo* species. K<sup>+</sup> conductance ( $g_K$ ) was highest in *L. pealei*, intermediate in *L. plei* and smallest in *S. sepioidea*. The time course and magnitude of  $g_K$  and  $g_{Na}$  were measured directly during membrane action potentials. These data reveal clear species-dependent differences in the amount of  $g_K$  and  $g_{Na}$  recruited during an action potential.

Key words: squid, giant axon, *Loligo pealei*, *Loligo opalescens*, *Loligo plei*, *Sepioteuthis sepioidea*, temperature adaptation, action potential, conduction velocity, K<sup>+</sup> conductance, Na<sup>+</sup> conductance, K<sup>+</sup> current, Na<sup>+</sup> current, conduction velocity, action potential broadening.

### Introduction

Hodgkin and Katz (1949) noted that 'The squid axon ceases to conduct at a temperature which is optimal for mammalian nerve, while isolated mammalian or tropical frog's nerves fail when cooled to a temperature at which the response of the squid axon reaches its maximum'. Action potentials, like many neurophysiological processes, e.g. synaptic transmission (Weight and Erulkar, 1976) but unlike ionic conduction, are highly temperature-sensitive. In spite of this, complex poikilotherms inhabit an extremely wide range of thermal environments, from -1.9 °C in the Antarctic to above 50 °C in certain hot springs (Macdonald, 1988). How do their nervous systems adapt? In response to this question, much attention has been focused at the level of the synapse (Prosser and Nelson, 1981). Relatively little effort has been directed at the action potential itself. This is particularly surprising given that almost 50 years ago, using the squid axon, Hodgkin and Huxley (1952) clearly identified those properties of the action potential that could be potential targets of temperature adaptation.

Those studies that have examined the temperature adaptation of the action potential have focused mainly on

conduction velocity. For example, compared with temperate taxa at an equivalent recording temperature, Antarctic teleosts have relatively rapid conduction velocities (Macdonald, 1981; MacDonald et al., 1988). The same is true for certain leg nerves in Arctic seagulls (Chatfield et al., 1953). In a few cases, other parameters have been examined (e.g. action potential duration; Lagerspetz and Talo, 1967). No reports, however, have identified the underlying physiological mechanisms for an adaptive change. For example, do species-dependent conduction velocities result from changes in the magnitude of  $g_{Na}$ , in  $I_{Na}$  kinetics or in the fiber's cable properties? These questions are hindered by several factors. First, most axons are too small to permit the use of voltage-clamp methods to study ionic conductances. In many preparations, individual neurons cannot be easily identified. Finally, apparent adaptive differences between dissimilar organisms may be a consequence of evolutionary distance.

The squid giant axon, long used to examine basic mechanisms of excitability, is also an ideal model for temperature adaptation. Its dimensions permit the measurement of both action potentials and the underlying ionic

conductances. Although giant neurons are present in other molluscs, most consist of large somata, not giant axons useful for studying impulse propagation. As a result of the isolation of mRNAs for a Na<sup>+</sup> channel and a delayed rectifier K<sup>+</sup> channel, molecular reagents are available for the giant axon system (Rosenthal and Gilly, 1993; Rosenthal et al., 1996). The ionic conductances in this preparation have been investigated intensely for almost 50 years and are very well described. Finally, the giant axon can be easily identified in many squid taxa whose representatives inhabit a wide range of habitats. This study takes advantage of four species within the family *Loliginidae* whose collective temperature range spans 20 °C. Our questions address how their propagated action potentials compare and whether differences correlate with a species' thermal environment. We also investigate the ionic basis for these differences.

## Materials and methods

### *Squid collection and dissection*

Four species of squid were used for these studies. Adult specimens of *Loligo opalescens* were collected from the Santa Monica Bay (near Los Angeles, California, USA) during January and February 1997 from waters at approximately 13 °C. Animals were maintained in recirculating seawater tanks at 12 °C for 1–3 days and used at UCLA. Specimens of *Loligo pealei* were collected adjacent to the Marine Biological Laboratory (MBL), Woods Hole, Massachusetts, USA, in May and August 1997 and in May 1998. In May, animals were caught in the shallow waters of the Woods Hole Passage (approximately 12–13 °C) and in August in somewhat deeper waters (10–20 m) of the Vineyard Sound, where data loggers placed next to the net opening measured water temperatures to be 18–20 °C. Squid were kept in flow-through seawater tanks at ambient water temperatures (10–18 °C) for 1–2 days. Specimens of both *L. plei* and *Sepioteuthis sepioidea* were collected near Mochima, Venezuela, during April 1998 and April and May 2000. *S. sepioidea* were caught over shallow reefs within Mochima Bay at 23.5–27.5 °C, and *L. plei* were jigged in deeper waters (approximately 20 m, 19–20.5 °C) near the bay's outer mouth. Both species were maintained in flow-through seawater tanks at 26–29 °C, and experiments were conducted at the Marine Station (Fundaciones Instituto Venezolano de Investigaciones Científicas, IVIC) in the village of Mochima, Sucre State, Venezuela.

Giant axons were isolated from adult specimens using standard methods. Squid were rapidly decapitated, and the hindmost stellar nerves were removed from the mantle and bathed in filtered sea water. Small nerve fibers and other connective tissue were manually removed from the giant fiber. In general, axons were used for experimentation immediately; however, in some cases, they were stored at 4 °C for 4–5 h. All experiments used 10K artificial sea water (10K ASW; in mmol<sup>-1</sup>: 430 NaCl, 10 KCl, 50 MgCl<sub>2</sub>, 10 CaCl<sub>2</sub>, 10 Hepes, pH 7.5, 970–980 mosmol<sup>-1</sup>).

### *Temperature control and measurements*

For all experiments, temperature was controlled using Peltier units, placed immediately under the recording chamber, driven by a standard temperature-control circuit. Temperatures were measured directly adjacent to the axon with a hand-held thermocouple and varied by no more than ±0.5 °C. Field temperature measurements were made with a Thermochron IButton data logger (Dallas Semiconductor, Dallas, TX, USA). The reported accuracy of this device is ±0.5 °C.

### *Propagated action potential measurements*

The details of propagated action potential measurements have been described previously (Rosenthal and Bezanilla, 2000b). In brief, 4–6 cm lengths of axon were mounted in a rectangular glass chamber. Action potentials were stimulated at one end of the axon by brief current pulses (2–20 μA for 200–400 μs) delivered through an intracellular micropipette (0.4–0.6 MΩ) connected to the ±10 V output of the on-line D/A converter. Recordings were made at two points along the axon with intracellular glass microelectrodes (1–3 MΩ) connected to capacity-compensated, high-impedance electrometers. The chamber was grounded through two Ag/AgCl coils embedded in 10K ASW containing 3% agarose and connected to the amplifier's virtual ground. Signals were digitized at rates between 200 kHz and 1 MHz (depending on the chamber temperature) using a PC44 signal processor board (Innovative Integration, Simi Valley, CA, USA) and a PC-compatible computer. Data were filtered at 1/10th the sampling rate and analyzed using software written in our laboratory. A calibrated eyepiece micrometer was used to measure each axon's diameter and the distance between electrodes. Only electrode impalements that displayed resting potentials more hyperpolarized than –55 mV were considered for analysis. In all experiments, axons were bathed in 10K ASW.

### *Voltage-clamp measurements*

The voltage-clamp apparatus utilized in these studies has been described previously in greater detail (Bezanilla et al., 1982a,b; Rosenthal and Bezanilla, 2000b). In general, transmembrane voltage was measured with two reference electrodes. The external reference, a wide-bore glass capillary, was positioned adjacent to the axon's mid-point. The internal reference, a capillary approximately 50–70 μm in diameter, containing a floating 25 μm platinum wire threaded along its entire length, was inserted into the axon from one end and advanced until its tip reached the mid-point. Voltage was clamped by passing currents through a platinized platinum wire inserted down the axon's entire length. The diameter of this wire was normally 75 μm, but for many small axons (<325 μm in diameter) a 50 μm wire was used. Data were collected as described in the previous section. As before, 10K ASW was used as external solution and native axoplasm served as the internal solution.

For voltage-clamp experiments that did not involve instantaneous interruptions of the action potential, signals were leak-subtracted using a standard P/–4 procedure

(Bezanilla and Armstrong, 1977). Holding potentials were either  $-65$  or  $-70$  mV.  $K^+$  currents were studied by applying tetrodotoxin (TTX) to the bath.  $Na^+$  currents were isolated by subtracting the  $K^+$  current ( $I_K$ ) from total membrane currents. To block all inward current activated by a brief pulse to 0 mV,  $200 \text{ nmol l}^{-1}$  TTX was added. In our hands, TTX subtraction was adequate for studying time points prior to and including peak  $Na^+$  current ( $I_{Na}$ ), a time range when very little  $I_K$  was activated. This permitted the measurement of peak  $Na^+$  conductance ( $g_{Na}$ ) and its activation kinetics. At later time points, after substantial  $I_K$  had been activated, this method became less reliable because of subtraction artifacts. Accordingly, the inactivation kinetics of  $I_{Na}$  was not studied.

Our experimental apparatus was modified slightly for action potential interruptions. To generate the action potential, the axial wire was connected to the output of the current generator and to the output of the control amplifier of the voltage-clamp through an electronic switch (FET switch with TTL input). To switch the voltage-clamp on suddenly, a TTL pulse activated this switch connecting the output of the control amplifier to the axial wire, while the same pulse opened another electronic switch removing an auxiliary feedback loop across the control amplifier. Membrane action potentials were triggered on-line in current-clamp mode by passing brief (approximately  $200 \mu\text{s}$ ) current pulses through the axial wire using a battery-powered stimulator. At timed intervals, the current-clamp was changed rapidly to voltage-clamp by activating the switches with TTL pulses generated under computer control. The speed of this transition was assessed by monitoring the voltage signal, and voltages were clamped to their command values within approximately  $10 \mu\text{s}$ . For  $I_{Na}$  experiments, action potentials were interrupted every  $20\text{--}50 \mu\text{s}$  by clamping to the  $K^+$  equilibrium potential ( $E_K$ ). For  $I_K$  experiments, action potentials were interrupted every  $100$  or every  $200 \mu\text{s}$  by clamping to the  $Na^+$  equilibrium potential ( $E_{Na}$ ). Instantaneous current values were measured immediately after the clamp had settled. Axons were held at  $-60$  mV.

#### Data analysis

For propagated action potentials, rise times and fall times were measured between 10 and 90% of the action potential's peak value. In experiments using two microelectrodes, conduction velocities were computed by dividing the distance separating the two electrodes by the time between the peak of the action potential passing each point. Measurements were then normalized by the square root of the axon's diameter (Hodgkin and Huxley, 1952; Taylor, 1963). For voltage-clamped axons, the time taken for either  $I_K$  or  $I_{Na}$  to reach half its maximal value after a voltage step was used as an index of activation kinetics.  $K^+$  conductance ( $g_K$ ) was computed by dividing the instantaneous current measured between the end of a voltage pulse (where  $I_K$  was fully activated) and the return to rest by the magnitude of the voltage difference at the same points. For  $g_{Na}$ , peak  $I_{Na}$  was measured and divided by the magnitude of the voltage step minus  $E_{Na}$ . For action potential interruption experiments, both  $g_K$  and  $g_{Na}$  were measured

using the second method. Leak subtraction for interruption experiments was performed manually. For  $I_K$  interruptions, current was measured following an instantaneous voltage jump to  $E_{Na}$  in the absence of a stimulated action potential. This current was then subtracted from experimental values. For  $I_{Na}$  interruptions, the same strategy was employed except that voltages were jumped to  $E_K$ . For all experiments,  $g_K$  and  $g_{Na}$  were normalized to the axon's surface area. Surface areas were estimated by visually measuring the axon's average diameter and assuming the geometry to be that of a cylinder. This approach assumes that membrane infoldings, if present, were equivalent for the axons of each species.

## Results

The squid species for this study were captured from different sites. In all cases, environmental temperatures were recorded as accurately as possible; a more detailed treatment of each species' natural temperature range can be found in the Materials and methods and Discussion sections. The collective temperature range for the squid used in this study spans approximately  $20^\circ\text{C}$ .

#### Propagated action potential measurements

Like most physiological processes, propagated action potentials are temperature-sensitive. For example, in squid axons, conduction velocities have a  $Q_{10}$  of less than 2, and the temperature-sensitivities of the rise times and fall times are significantly steeper, i.e.  $Q_{10}$  values are greater than 2 (Chapman, 1967; Hodgkin and Katz, 1949; Rosenthal and Bezanilla, 2000b).

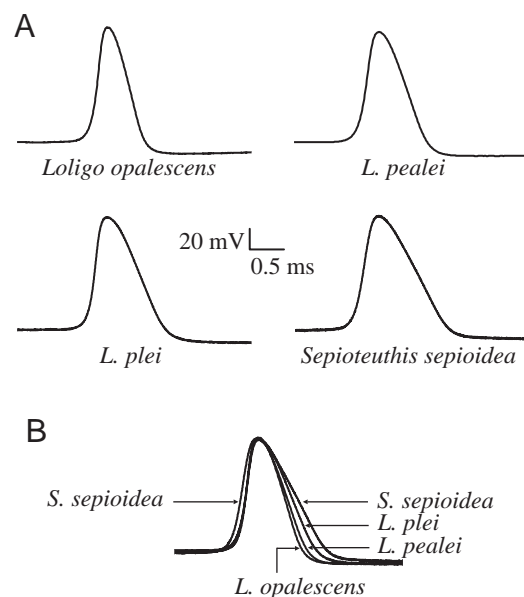


Fig. 1. Propagated action potentials from the giant axons of four species of squid. Single propagated action potentials were recorded from giant axons using intracellular microelectrodes. (A) Action potentials from four species. (B) Action potentials from A superimposed by aligning peaks. All recordings were made at  $15^\circ\text{C}$ . Axons were bathed in 10K ASW (see Materials and methods).

To investigate whether any of these properties correlate with the squid's thermal environment, recordings were made from axons of each of the four species identified above. Fig. 1A shows examples of these recordings taken at 15 °C. In each case, action potentials are characterized by rapid voltage changes of more than 100 mV, followed by a typical undershoot. A casual inspection of the recordings indicates that the action potential duration is variable, being greater in *S. sepioidea* than in *L. opalescens*. In Fig. 1B, the action potentials have been superimposed by aligning their peaks. Clearly, the duration of the falling phase differs among all four recordings and correlates with each species' thermal environment: warmer environments are associated with slower fall times. The rise time, in contrast, shows a different pattern: the rise times for all species of *Loligo* are equivalent and are faster than those for *S. sepioidea*.

By averaging many experiments, each recorded over a large temperature range, we examined in detail the species-dependent features of the action potentials (Fig. 2). The three parameters investigated are depicted in Fig. 2A. The rise times for all species of *Loligo* are equivalent (Fig. 2B). Those for *S. sepioidea*, however, are on average 44% slower at each temperature. The fall times (Fig. 2C) are different for all species and can be ranked from fastest to slowest as follows: *L. opalescens* < *L. pealei* < *L. plei* < *S. sepioidea*. The relative differences tend to increase at lower temperatures and are particularly apparent below approximately 7.5 °C. As with rise times, conduction velocities are equivalent for all *Loligo* species but different from that of *S. sepioidea*. At temperatures below 10 °C, *Loligo* conduction velocities are up to 100% faster, whereas above 10 °C they are approximately 50%

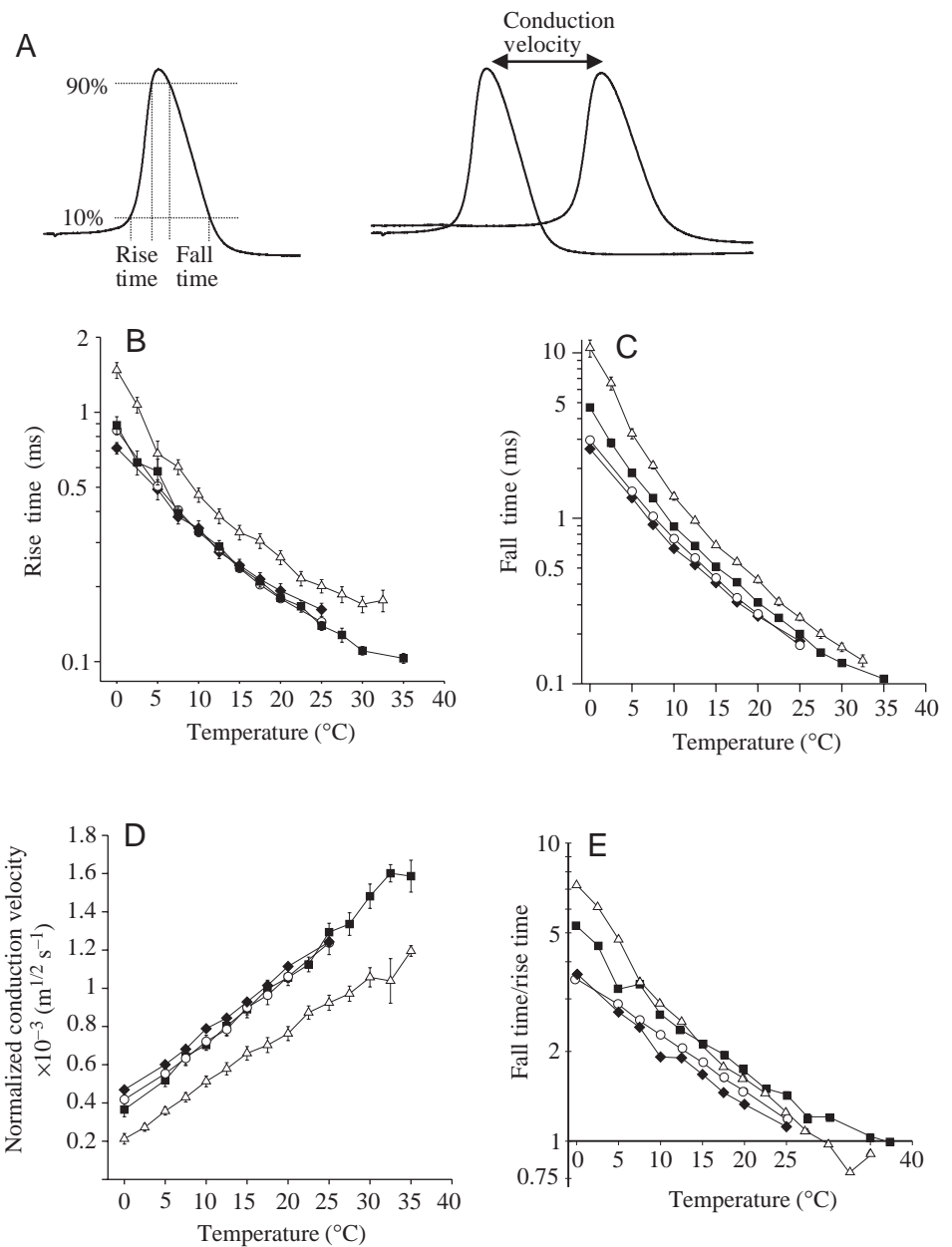


Fig. 2. Analysis of propagated action potentials. Measurements of propagated action potential rise time, fall time and conduction velocity in four species of squid.  $\blacklozenge$ , *Loligo opalescens*;  $\circ$ , *L. pealei*;  $\blacksquare$ , *L. plei*;  $\triangle$ , *Sepioteuthis sepioidea*. Values are means  $\pm$  S.E.M. (A) Schematic diagram of how measurements were made. Both rise time and fall time were measured between 10 and 90% of the voltage difference between rest and action potential peak. Conduction velocities were taken from experiments using two electrodes, and velocities were measured by dividing the distance between the electrodes by the time between the two action potential peaks. (B) Graph of rise time versus temperature. The ordinate is plotted on a logarithmic scale. *L. opalescens*,  $N=6$ ; *L. pealei*,  $N=18$ ; *L. plei*,  $N=9$ ; *S. sepioidea*,  $N=9$ . (C) Graph of fall time versus temperature. The ordinate is plotted on a logarithmic scale. *L. opalescens*,  $N=6$ ; *L. pealei*,  $N=19$ ; *L. plei*,  $N=9$ ; *S. sepioidea*,  $N=9$ . (D) Graph of conduction velocity versus temperature. Conduction velocities were normalized to the square root of the axon's diameter. *L. opalescens*,  $N=4$ ; *L. pealei*,  $N=11$ ; *L. plei*,  $N=5$ ; *S. sepioidea*,  $N=6$ . (E) Ratio of fall time to rise time versus temperature (data from B and C).

Table 1.  $Q_{10}$  values of action potential rise times, fall times and conduction velocities from four squid species

Species	Action potential parameter	$Q_{10}$		
		0–10 °C	10–20 °C	20–30 °C
<i>Loligo opalescens</i>	Rise time	2.10	1.78	1.42*
	Fall time	4.00	2.57	2.00*
	Conduction velocity	1.68	1.41	1.24*
<i>L. pealei</i>	Rise time	2.56	1.85	1.54*
	Fall time	3.94	2.85	2.39*
	Conduction velocity	1.73	1.47	1.36*
<i>L. plei</i>	Rise time	2.66	1.85	1.63
	Fall time	5.25	2.88	2.32
	Conduction velocity	1.92	1.50	1.40
<i>Sepioteuthis sepioidea</i>	Rise time	3.16	1.78	1.54
	Fall time	7.90	3.19	2.55
	Conduction velocity	2.42	1.49	1.39

\*Based on measurements at 20 and 25 °C.

faster. The temperature-sensitivities ( $Q_{10}$ ) of these processes also vary (Table 1). For each species, the  $Q_{10}$  values of the fall times are large and those of the conduction velocities are relatively small. In general,  $Q_{10}$  values are highest over the lowest temperature range (0–10 °C). This feature is particularly exaggerated for *S. sepioidea*, in which the  $Q_{10}$  for the fall time is 7.9 compared with approximately 4 for the two temperate species of *Loligo*. That for *L. plei*, at 5.25, is intermediate. Over higher temperature ranges, the  $Q_{10}$  values for these processes are more similar.

The temperature limits of the propagated action potential were also studied. No low-temperature block was encountered: all species were able to generate action potentials down to 0 °C. However, action potential failure was readily apparent at high temperatures, and the temperature varied among species. For *L. pealei* and *L. opalescens*, action potentials failed at  $29.5 \pm 0.8$  °C ( $N=9$ ) and  $29.0 \pm 0.2$  °C ( $N=3$ ) respectively. For *L. plei* and *S. sepioidea*, failure temperatures were significantly higher:  $37.8 \pm 1.3$  °C ( $N=4$ ) and  $34.9 \pm 0.6$  °C ( $N=6$ ; means  $\pm$  S.E.M.) respectively. In all experiments, action potentials could be recovered by lowering the temperature. Interestingly, the failure temperature is reflected in the ratio of the fall time to the rise time (Fig. 2E). Because of the relatively high  $Q_{10}$  of the fall time, this ratio decreases as the temperature increases. As this ratio reaches unity, it is increasingly likely that the action potential will fail. In the case of *S. sepioidea*, action potentials were measured in which fall times were slightly faster than rise times, but in axons of *Loligo* failure occurred prior to this point. As with the measurements of the absolute failure temperatures, the fall time:rise time ratio in *S. sepioidea* and *L. plei* axons is shifted to the right on the temperature axis.

The preceding analysis of propagated action potentials indicated that both rise times and conduction velocities were similar among *Loligo* species, but slower in *S. sepioidea*. By contrast, all species exhibited different fall times. These results suggest that some specific property of the  $\text{Na}^+$  conductance

may differ between *S. sepioidea* and the *Loligo* species, and that the  $\text{K}^+$  conductance may differ among all species. However, the analysis cannot predict which physiological property of a particular conductance will vary. For example, changes in kinetics, voltage-dependence or absolute conductance level could bring about similar results.

#### Voltage-clamp measurements

To examine  $g_{\text{K}}$  and  $g_{\text{Na}}$  directly, voltage-clamp experiments were performed. Axons from all species except *L. opalescens* were compared under identical conditions. Specimens of *L. opalescens* were excluded because the axons of most specimens were too small for this technique. Fig. 3A shows a typical voltage-clamp current recording following a 3.5 ms pulse to 0 mV from an *S. sepioidea* axon. The general features of this current were shared by all species. In squid axons, a rapidly activating inward current is carried by  $\text{Na}^+$  ( $I_{\text{Na}}$ ), and a delayed outward current is carried by  $\text{K}^+$  ( $I_{\text{K}}$ ) (Hodgkin and Huxley, 1952).  $I_{\text{K}}$  can be isolated by adding TTX to the bath. In Fig. 3B, the same axon has been treated with TTX, and a family of classic ‘delayed rectifier’  $\text{K}^+$  currents is shown. Their characteristic shape is derived from rapid activation following a pronounced delay.  $I_{\text{Na}}$  was more complicated to study. Fig. 3Ci shows two currents traces from an *L. plei* axon after a voltage step to –10 mV before and after the addition of TTX. The TTX-sensitive current, visualized by subtracting these two recordings, was considered to be  $I_{\text{Na}}$  (Fig. 3Cii).  $I_{\text{Na}}$  of squid axons activates very rapidly, with a much shorter delay than  $I_{\text{K}}$ , and then inactivates with a quasi-exponential time course. It is noteworthy that, when  $I_{\text{Na}}$  is at its peak, virtually no  $I_{\text{K}}$  has activated (Fig. 3Ci). This relationship held irrespective of the voltage, temperature or species (data not shown). At later times, increasingly larger proportions of  $I_{\text{K}}$  had to be subtracted. In some axons, this process introduced artifacts in the time course of  $I_{\text{Na}}$  inactivation. For this reason, analysis focused on activation kinetics and maximal conductance. A

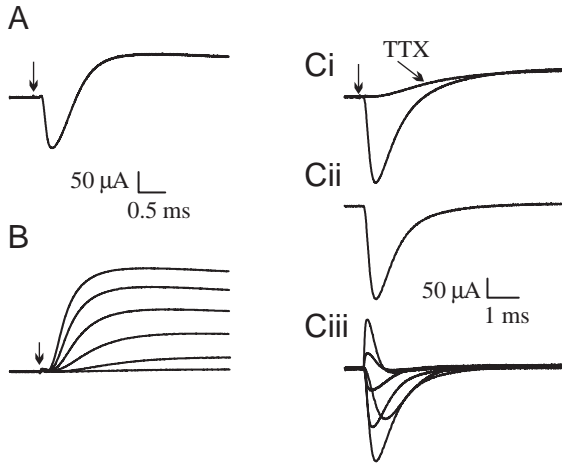


Fig. 3. Separation of  $\text{Na}^+$  and  $\text{K}^+$  currents from voltage-clamped axons. (A) Voltage-clamp recording from a *Sepioteuthis sepioidea* axon at  $20^\circ\text{C}$ . The arrow indicates the start of a voltage step to  $0\text{ mV}$ . (B) Family of  $\text{K}^+$  currents from a *S. sepioidea* axon at  $20^\circ\text{C}$  in the presence of tetrodotoxin (TTX). At the arrow, voltages were stepped from the holding potential to  $-40\text{ mV}$ ,  $-20\text{ mV}$ ,  $0\text{ mV}$ ,  $20\text{ mV}$ ,  $40\text{ mV}$  and  $60\text{ mV}$ . (C) Measurement of  $\text{Na}^+$  current ( $I_{\text{Na}}$ ) in a *Loligo plei* axon at  $10.6^\circ\text{C}$  by TTX subtraction. (i) Two traces after voltages had been stepped from the holding potential to  $-10\text{ mV}$ , before and after TTX, superimposed. (ii)  $I_{\text{Na}}$  resulting from the TTX trace being subtracted from non-TTX trace. (iii) A family of  $I_{\text{Na}}$  traces from the same axon, using the same technique, after voltage steps to  $-30\text{ mV}$ ,  $-10\text{ mV}$ ,  $10\text{ mV}$ ,  $30\text{ mV}$ ,  $50\text{ mV}$  and  $70\text{ mV}$ . All holding potentials were  $-70\text{ mV}$ . The external solution was  $10\text{K ASW}$  (see Materials and methods). The first points of each trace are at  $0\text{ }\mu\text{A}$ .

family of subtracted  $\text{Na}^+$  currents, recorded at various voltages, is shown in Fig. 3Ciii. In this case, currents activate rapidly even after modest depolarizations, and their direction reverses between approximately  $+30$  and  $+50\text{ mV}$ . The following analysis is based on  $I_{\text{K}}$  and  $I_{\text{Na}}$  recorded from all three species in an analogous manner.

Steady-state and kinetic parameters of  $g_{\text{Na}}$  and  $g_{\text{K}}$  were analyzed for all species, and these results are presented in Fig. 4. Clearly, the most striking difference rests in the absolute levels of  $g_{\text{Na}}$  and  $g_{\text{K}}$ . For both species of *Loligo*,  $g_{\text{Na}}$  reaches a maximum of approximately  $75\text{ mS cm}^{-2}$  at voltages greater than  $+10\text{ mV}$  (Fig. 4A). In *S. sepioidea* axons,  $g_{\text{Na}}$  reaches only  $47\text{ mS cm}^{-2}$  (approximately 63% of the value for the *Loligo* species). Maximal  $g_{\text{K}}$ , however, is different for all three species: for *L. pealei*, *L. plei* and *S. sepioidea*, the corresponding values are  $73\text{ mS cm}^{-2}$ ,  $54\text{ mS cm}^{-2}$  (approximately 74% of the value for *L. pealei*) and  $38\text{ mS cm}^{-2}$  (approximately 52%), respectively. These differences are highly significant (see figure legend). In Fig. 4C,D, values of  $g_{\text{Na}}$  and  $g_{\text{K}}$  have been normalized to their maximum values and then plotted against voltage. In both cases, the conductances activate steeply between approximately  $-30\text{ mV}$  and  $+20\text{ mV}$ . The  $g_{\text{Na}}$ /voltage relationship is particularly steep. In neither case, however, is there a significant inter-species difference in voltage-dependence. Activation kinetics for both currents were also

equivalent among species. The half-time ( $t_{1/2}$ ) for activation versus voltage relationships for both  $I_{\text{Na}}$  and  $I_{\text{K}}$  are shown in Fig. 4E,F. In general,  $I_{\text{Na}}$  activated approximately 10 times faster than  $I_{\text{K}}$ . For both  $I_{\text{Na}}$  and  $I_{\text{K}}$ , half-times for activation were not statistically different among species. All results in Fig. 4 were taken from axons at  $10^\circ\text{C}$ . Similar experiments conducted at  $20^\circ\text{C}$  yielded the same relative results (not shown).

#### Conductance measurements during the action potential

Data from voltage-clamped axons suggest that differences in absolute conductance levels are consistent with species-specific differences in the propagated action potential. Accordingly, slower action potential rise times for *S. sepioidea* are due to a smaller  $g_{\text{Na}}$ ; differences in fall times between all three species are due to different levels of  $g_{\text{K}}$ . These hypotheses were tested directly by reconstructing the time course and magnitude of  $g_{\text{Na}}$  and  $g_{\text{K}}$  during membrane action potentials. The strategy was to stimulate action potentials in current-clamped axons and then to 'interrupt' them at specific times by rapidly switching to voltage-clamp mode. If the voltage is clamped to the  $\text{K}^+$  equilibrium potential ( $E_{\text{K}}$ ), then the resulting instantaneous current jump is due to  $I_{\text{Na}}$ . Conversely, if the voltage is clamped to the  $\text{Na}^+$  equilibrium potential ( $E_{\text{Na}}$ ), then the current is due to  $I_{\text{K}}$ . Thus, by interrupting the action potential at many points, the time course of both  $g_{\text{Na}}$  and  $g_{\text{K}}$  can be measured. The method of action potential interruption, along with the underlying assumptions, has been described in greater detail previously (Bezanilla et al., 1970; Rojas et al., 1970).

It is assumed that, early during an action potential, the reversal potential ( $E_{\text{rev}}$ ) corresponds to  $E_{\text{Na}}$ , and later to  $E_{\text{K}}$  (when  $I_{\text{Na}}$  or  $I_{\text{K}}$  is large, small leak conductances have a minimal contribution; see above references). Therefore, to determine  $E_{\text{Na}}$  and  $E_{\text{K}}$ ,  $E_{\text{rev}}$  was measured at different times during an action potential. Fig. 5 demonstrates an example of this type of experiment. Fig. 5A shows a typical membrane action potential, in this case recorded from a *L. pealei* axon at  $15^\circ\text{C}$ . In Fig. 5Bi, seven action potentials, from the same axon, have been superimposed. In each case, the voltage-clamp was activated after  $700\text{ }\mu\text{s}$  and the membrane was clamped to a different potential ( $-70\text{ mV}$  to  $+50\text{ mV}$  in increments of  $20\text{ mV}$ ). Fig. 5Bii shows the resulting current traces. All the following results focus on the magnitude of the instantaneous current jump after the voltage-clamp has been activated and the voltage has settled to its new value. The relationship between this current and voltage ( $I/V$ ) was used to determine  $E_{\text{rev}}$ . In this case,  $E_{\text{rev}}$  was  $-27\text{ mV}$  (due to activation of both  $g_{\text{Na}}$  and  $g_{\text{K}}$ ). Fig. 5C shows a time series of  $E_{\text{rev}}$  determinations plotted on top of an action potential. In this case,  $E_{\text{rev}}$  begins at approximately  $+55\text{ mV}$  and, by the end of the action potential, reaches approximately  $-70\text{ mV}$ . The maximum and minimum values are taken to be  $E_{\text{Na}}$  and  $E_{\text{K}}$ , respectively. Similar experiments were repeated for each species, and no significant differences were found among species for either  $E_{\text{Na}}$  or  $E_{\text{K}}$ .

Values of  $E_{\text{Na}}$  and  $E_{\text{K}}$  were then used to examine the time course of  $g_{\text{Na}}$  and  $g_{\text{K}}$  during an action potential (Fig. 6). Fig.

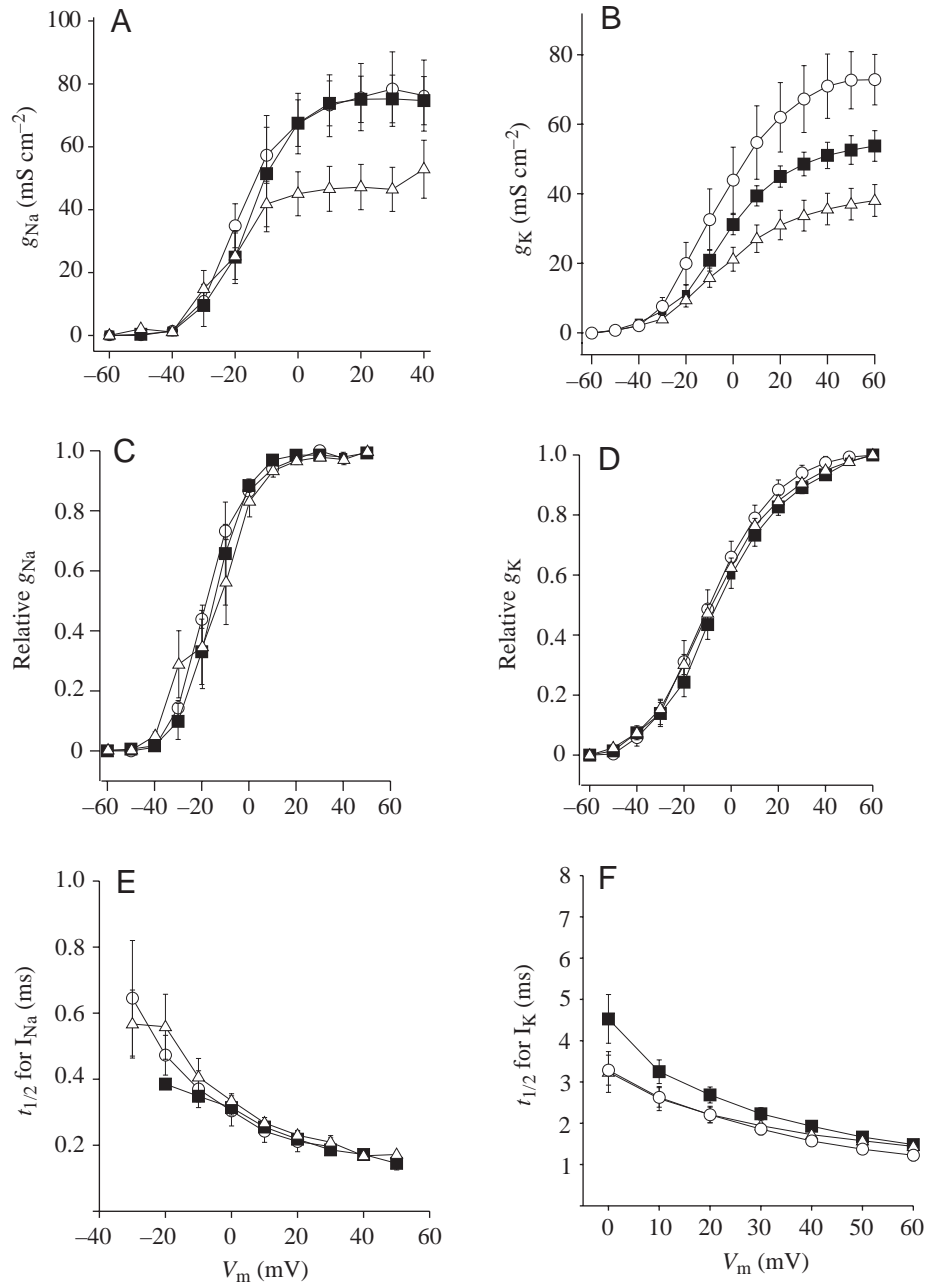


Fig. 4. Analysis of Na<sup>+</sup> conductance ( $g_{Na}$ ) and K<sup>+</sup> conductance ( $g_K$ ) from voltage-clamped axons. All analyses are derived from experiments at 10 °C. ○, *L. pealei*; ■, *L. plei*; △, *Sepioteuthis sepioidea*. Values are means ± S.E.M. (A)  $g_{Na}$ , normalized to membrane surface area, versus voltage. *L. pealei*,  $N=5$ ; *L. plei*,  $N=5$ ; *S. sepioidea*,  $N=9$ . Values for *S. sepioidea* are significantly different ( $P \leq 0.05$ ) from those for either species of *Loligo* between 0 mV and +30 mV (at +40 mV,  $P=0.06$ ). (B)  $g_K$ , normalized to membrane surface area, versus voltage. *L. pealei*,  $N=5$ ; *L. plei*,  $N=7$ ; *S. sepioidea*,  $N=8$ . Values are significantly different between *L. plei* and *L. pealei* at all voltages  $\geq +20$  mV and between *L. plei* and *S. sepioidea* at all voltages  $\geq 0$  mV. (C)  $g_{Na}$ , normalized to maximum values of  $g_{Na}$ , versus voltage. (D)  $g_K$ , normalized to maximum values of  $g_K$ , versus voltage. (E) Half-time ( $t_{1/2}$ ) for  $I_{Na}$  versus voltage. (F)  $t_{1/2}$  for  $I_K$  versus voltage.  $t_{1/2}$  was defined as the time after the voltage step when half the maximum current was activated.  $V_m$ , membrane potential.

6Ai shows an ‘interrupted’ action potential from an *L. pealei* axon at 10 °C. In this case, the action potential is clamped after 700  $\mu$ s (arrow) to  $-70$  mV ( $E_K$ ). The resultant  $I_{Na}$  is shown in Fig. 6Aii. At the time the clamp is activated, the current jumps almost instantaneously from near 0  $\mu$ A to approximately 375  $\mu$ A, after which  $I_{Na}$  rapidly deactivates back to 0  $\mu$ A. Thus, the instantaneous current jump is proportional to  $g_{Na}$  at 700  $\mu$ s. Here,  $g_{Na}$  is 3.0 mS. A similar experiment, designed to measure  $g_K$ , is illustrated in Fig. 6Bi. In this case, the action potential is interrupted after 2 ms and clamped to +55 mV ( $E_{Na}$ ). Upon clamping, the current (Fig. 6Bii) jumps from near zero to approximately 173  $\mu$ A. Thus,  $g_K$  at 2 ms is 1.4 mS.

These procedures, conducted at many time points, were extended to each species, and the complete time courses for

both  $g_{Na}$  and  $g_K$  were determined (Fig. 6C–E). In each case,  $g_{Na}$  activates rapidly and reaches its peak simultaneously with that of the action potential.  $g_K$  activates less steeply and with a pronounced delay, reaching its peak after the action potential has almost fully repolarized. Several features, however, differ between the data presented in Fig. 6C–E. First, peak  $g_K$  is greatest in *L. pealei* (approximately 29 mS cm<sup>-2</sup>), intermediate in *L. plei* (approximately 23 mS cm<sup>-2</sup>) and smallest in *S. sepioidea* (approximately 19 mS cm<sup>-2</sup>). Peak  $g_{Na}$ , in contrast, is greatest in *L. plei* (approximately 65 mS cm<sup>-2</sup>), intermediate in *L. pealei* (approximately 50 mS cm<sup>-2</sup>) and smallest in *S. sepioidea* (approximately 44 mS cm<sup>-2</sup>). In addition,  $g_K$  appears to turn on and off faster in *L. pealei* than in the other two species.  $g_{Na}$ , in contrast, activates extremely rapidly in each

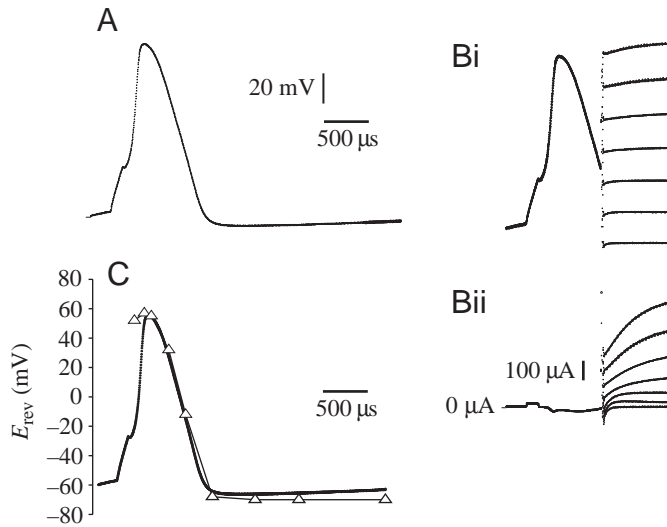


Fig. 5. Measurement of the reversal potential during a membrane action potential. All recordings were taken from a *Loligo pealei* axon at 15 °C. Holding potential, just before current clamping, was  $-65$  mV. Axons were bathed in 10K ASW (see Materials and methods). (A) A single membrane action potential. (Bi) Seven similar action potential recording, which have been voltage-clamped after  $700\ \mu\text{s}$ , superimposed. Voltage-clamp potentials are from  $-70$  mV to  $+50$  mV in increments of  $20$  mV. (Bii) Paired current traces for voltage traces in Bi demonstrating instantaneous jumps. (C) Results from nine experiments similar to that in B but interrupted at different times. Reversal potential ( $E_{\text{rev}}$ ), determined from instantaneous current/voltage plots, plotted as a function of time and superimposed onto an action potential.

case. It turns off, however, more rapidly in *L. pealei* than in the other two species. These findings are based on data from a single representative axon for each species. Because of variation among axons, these studies were extended to multiple axons from each species.

Fig. 7 shows mean  $g_{\text{Na}}$  and  $g_{\text{K}}$  for each species. Because the stimulus duration and action potential latency varied slightly among axons, all time points were normalized using the action potential's peak as time zero. Fig. 7A demonstrates that, contrary to the results presented in Fig. 6, absolute  $g_{\text{Na}}$  is equivalent for both *Loligo* species, reaching approximately  $55\ \text{mS cm}^{-2}$  as the action potential peaks. In *S. sepioidea*, peak  $g_{\text{Na}}$  is significantly smaller (approximately  $37\ \text{mS cm}^{-2}$ ; 67% of the value for the *Loligo* species;  $P \leq 0.05$ ). In Fig. 7B,  $g_{\text{Na}}$  measurements have been normalized to their peak values to compare kinetics. Although  $g_{\text{Na}}$  appears to peak slightly more slowly in *S. sepioidea*, there are no significant differences in activation. The time course of the falling phase does differ among species, being fastest in *L. pealei*, intermediate in *L. plei* and slowest in *S. sepioidea*. This is expected because, during the action potential, the turning off of  $g_{\text{Na}}$  is driven mainly by the turning on of  $g_{\text{K}}$ , which is fastest in *L. pealei* and slowest in *S. sepioidea*. Unlike  $g_{\text{Na}}$ , maximum  $g_{\text{K}}$  differs among species. It is greatest in *L. pealei* (approximately  $36\ \text{mS cm}^{-2}$ ), intermediate in *L. plei* (approximately  $24\ \text{mS cm}^{-2}$ ;

66% of the value for *L. plei*) and smallest in *S. sepioidea* (approximately  $17\ \text{mS cm}^{-2}$ ; 47%). The kinetics of  $g_{\text{K}}$  (Fig. 7D) is indistinguishable between *L. plei* and *S. sepioidea*, but for *L. pealei* both the on and off rates are relatively fast. Thus, as with voltage-clamp experiments, absolute conductances show dramatic interspecies differences.

## Discussion

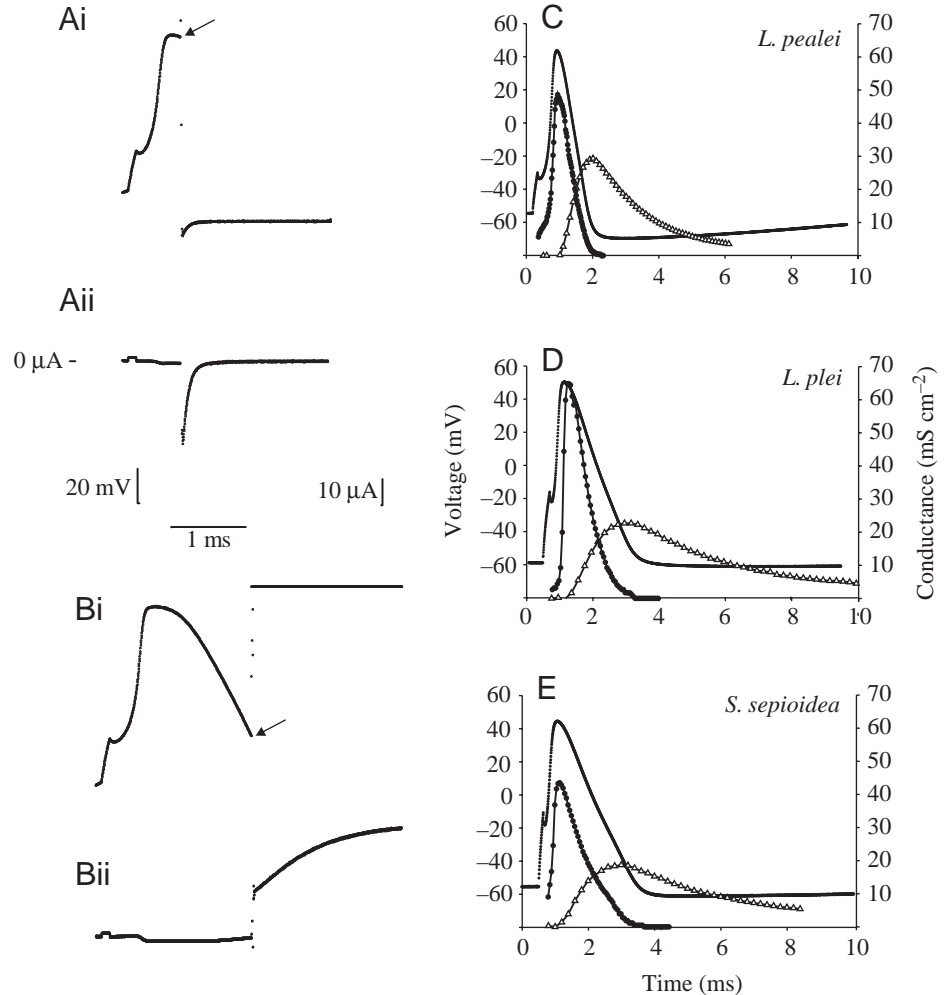
These investigations assume that the four test species inhabit different thermal environments. It is therefore appropriate to comment on the magnitude of this temperature range. At the outset, it should be stressed that the precise temperature range for these species is not known, a common problem for marine organisms. Geographically distinct subpopulations probably experience temperature variation as well. For the present purpose, we intend only to establish that each species' temperature range is different and that collectively they span approximately  $20\ ^\circ\text{C}$ .

*L. opalescens* is commonly found off the Pacific coast of North America and is particularly abundant off California. In the winter, populations are found in southern California, whereas for the rest of the year they are found off northern and central California. In both cases, surface temperatures rarely exceed  $13\ ^\circ\text{C}$  and are often several degrees lower. These squid have also been observed below the thermocline at temperatures as low as  $6\text{--}7\ ^\circ\text{C}$  (Neumeister et al., 2000). Specimens of *L. pealei* are commonly encountered off the Atlantic coast of North America from the Gulf of Maine to the Gulf of Mexico. Their temperature range has been discussed in greater detail elsewhere (Boyle, 1983; Rosenthal and Bezanilla, 2000b). In Woods Hole, this squid is most commonly encountered between approximately  $10$  and  $20\ ^\circ\text{C}$ , although their abundance is greatest when water temperatures are at the low end of this range. They are reported actively to avoid temperatures below  $8\ ^\circ\text{C}$  (Summers, 1969). Specimens of *L. plei* are commonly found in the Gulf of Mexico and in the Caribbean Sea off northern South America. In Mochima, Venezuela, where the specimens for this study were collected, water temperatures at the capture site (and depth) were between  $18$  and  $20.5\ ^\circ\text{C}$ . In the Gulf of Mexico, these squid are often encountered in the same areas as *L. pealei*; however, the abundance of each species is stratified with depth. *L. plei* prefer warmer surface waters ( $<50$  m), whereas *L. pealei* prefer cooler, deeper waters (Hixon et al., 1980; Whitaker, 1978, 1980). *S. sepioidea* are normally found adjacent to shallow reefs in the Caribbean Sea and the Gulf of Mexico (Voss, 1956). In Mochima, where specimens were collected, data loggers indicated that daily temperatures fluctuated between  $23.5$  and  $27\ ^\circ\text{C}$  in April and May. In July and August, temperatures were significantly higher ( $26\text{--}29\ ^\circ\text{C}$ ). It should be noted that both *L. plei* and *S. sepioidea* were maintained at  $29\text{--}30\ ^\circ\text{C}$  in flowing seawater tanks for several days before use with no obvious detrimental effects.

The data presented in this report identify three properties of the propagated action potential that vary. First, the duration of



Fig. 6. Measurement of the  $K^+$  conductance ( $g_K$ ) and  $Na^+$  conductance ( $g_{Na}$ ) during a membrane action potential. All recordings were made at  $10^\circ\text{C}$ . Holding potential was  $-65\text{ mV}$ . Axons were bathed in 10K ASW (see Materials and methods). For  $g_K$  experiments, time points are at  $100\mu\text{s}$  intervals for *Loligo pealei* and at  $200\mu\text{s}$  intervals for *L. plei* and *Sepioteuthis sepioidea*. For  $g_{Na}$ , time points are at  $20\mu\text{s}$  intervals for *L. pealei* and at  $50\mu\text{s}$  intervals for *L. plei* and *S. sepioidea*. (Ai) Membrane action potential from *L. pealei* interrupted by voltage-clamp to  $-70\text{ mV}$  ( $K^+$  equilibrium potential,  $E_K$ ) after  $700\mu\text{s}$  (arrow). (Aii) Matching current recording. The value of the instantaneous current at the time of voltage-clamp switch-on corresponds to the  $Na^+$  current ( $I_{Na}$ ). (Bi) Membrane action potential from *L. pealei* interrupted by voltage-clamp to  $+55\text{ mV}$  ( $Na^+$  equilibrium potential,  $E_{Na}$ ) after  $2\text{ ms}$  (arrow). (Bii) Matching current recording. The value of the instantaneous current at the time of voltage-clamp switch-on corresponds to the  $K^+$  current ( $I_K$ ). (C–E) Experiments similar to those in A and B, performed at many ‘interruption’ points were used to derive time courses for  $g_K$  and  $g_{Na}$  from axons of *L. pealei*, *L. plei* and *S. sepioidea*. In each panel, an action potential (solid line) is superimposed on the time course for  $g_{Na}$  (●) and  $g_K$  (△).



the action potential's falling phase differs among all species tested and correlates with the thermal environment of the species; when measured at equivalent temperatures, action potentials from species that inhabit colder environments are shorter. Second, the action potential's rising phase is relatively slow in *S. sepioidea*, but equivalent in all three species of *Loligo*. Third, the same relationship holds true for the conduction velocity.

The absolute levels of  $g_K$  and  $g_{Na}$  are consistent with all three changes in the propagated action potential. It should be stressed that species-dependent conductances were measured using two independent sets of experiments (voltage-clamped axons and action potential interruptions) and both yielded comparable results. Clearly, an increase in  $g_K$  will decrease the duration of the action potential's falling phase, an assertion supported by the Hodgkin and Huxley model (data not shown). In fact, for a number of systems, the action potential's duration is regulated by changing the level of  $g_K$  (Chen et al., 1996; Kaab et al., 1996; Thuringer et al., 1996; Zhang and McBain, 1995). The relatively slow action potential rise time and conduction velocity in *S. sepioidea* axons are consistent with its low levels of  $g_{Na}$ . On the basis of the Hodgkin and Huxley model axon, the level of  $g_{Na}$  correlates well with conduction

velocity and rise time (Adrian, 1975; Hodgkin, 1975; Huxley, 1959). However, more quantitative extrapolations of conduction velocity and rise time, using our measured conductance values, were not attempted. Years of scrutiny have indicated that several aspects of the Hodgkin and Huxley model require further refinement to predict properties of conduction with sufficient accuracy for the present purposes (Armstrong and Bezanilla, 1977; Armstrong et al., 1973; Armstrong and Hille, 1998; Vandenberg and Bezanilla, 1991; Bezanilla, 2000; Bezanilla and Armstrong, 1977). For example, as seen in Fig. 6, at the action potential's peak, there is virtually no  $g_K$ , a result not predicted by the Hodgkin and Huxley equations using the original parameters (Hodgkin and Huxley, 1952).

There are many plausible mechanisms for regulating ionic conductances in the giant axon. The most straightforward would be to modify the surface expression of  $Na^+$  or  $K^+$  channels by transcriptional mechanisms, by translational mechanisms or by changing turnover rates. Conceivably, the unitary conductance of  $Na^+$  and  $K^+$  channels could also be regulated. No evidence supports or refutes any of these possibilities. Species-dependent differences in slow inactivation could also influence the available levels of ionic

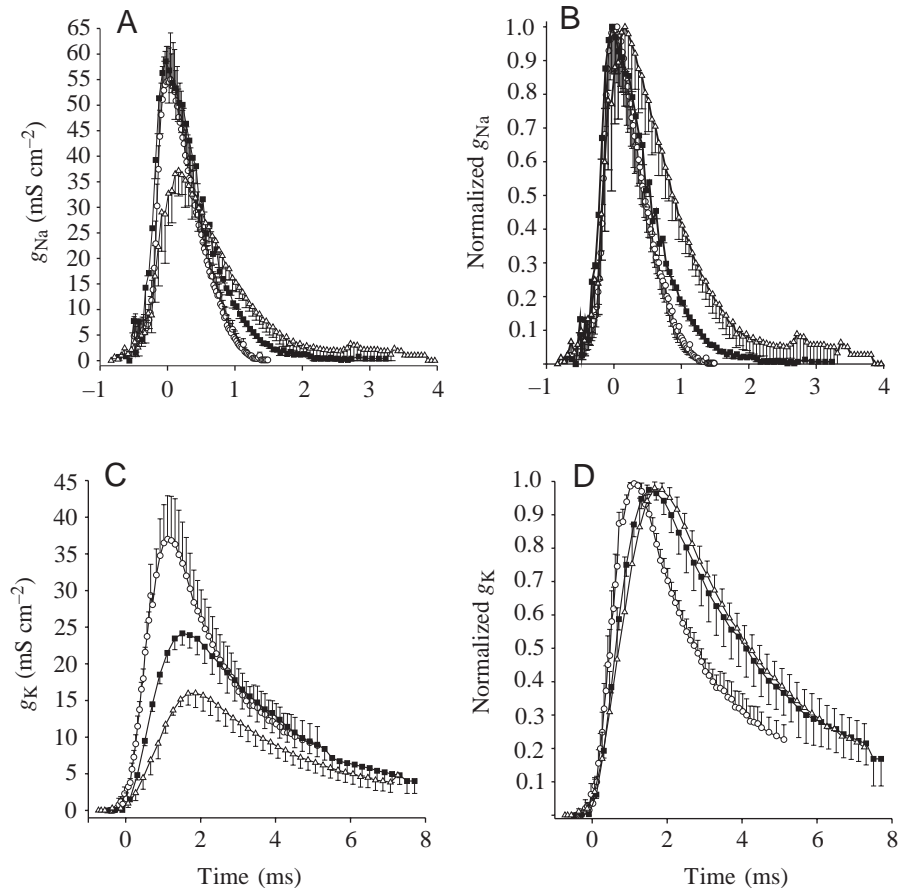


Fig. 7. Analysis of the  $K^+$  conductance ( $g_K$ ) and  $Na^+$  conductance ( $g_{Na}$ ) during a membrane action potential. All recordings were made at  $10^\circ\text{C}$ . The holding potential before current-clamp was  $-65\text{ mV}$ . Axons were bathed in 10K ASW (see Materials and methods).  $\circ$ , *L. pealei*;  $\blacksquare$ , *L. plei*;  $\triangle$ , *Sepioteuthis sepioidea*. Values are means  $\pm$  S.E.M. For all data, the action potential peak is considered to be time zero, and all time measurements are shifted accordingly. For  $g_K$  experiments, data points are at  $50\ \mu\text{s}$  intervals for *L. pealei* and at  $200\ \mu\text{s}$  intervals for *L. plei* and *S. sepioidea*. For  $g_{Na}$ , time points are at  $20\ \mu\text{s}$  intervals for *L. pealei* and at  $50\ \mu\text{s}$  intervals for *L. plei* and *S. sepioidea*. (A) Time course of  $g_{Na}$  (per surface area) versus time.  $N=5$  for all species. (B)  $g_{Na}$  normalized to peak values versus time (same data as in A). (C) Time course of  $g_K$  (per surface area) versus time.  $N=4$  for all species. (D)  $g_K$  normalized to peak values versus time (same data as in C).

conductances. However, at the holding potentials used for these studies ( $\leq -65\text{ mV}$ ), no significant slow inactivation was apparent for any species. For  $g_K$ , regulation may also be at the level of subunit assembly. Recent evidence suggests that  $\text{SqK}_V1.1A$ , a  $K^+$  channel mRNA that is thought to underlie some or all of delayed rectifier  $g_K$  in the giant axon (Rosenthal et al., 1996), contains several anomalous amino acid residues in a channel domain (T1) responsible for subunit tetramerization (Liu et al., 2001). The amino acids at these positions, which are regulated by RNA editing (Rosenthal and Bezanilla, 2000a), strongly influence the functional expression of heterologously expressed channels in *Xenopus* oocytes. Further evidence suggests that the pattern of RNA editing in the T1 domain of  $\text{SqK}_V1.1A$  varies among different species of squid (Rosenthal and Bezanilla, 1998).

The conductance level changes identified in this study are a plausible regulatory mechanism for the changes observed in the propagated action potentials. However, other possibilities exist. For example, inactivation and deactivation of  $g_{Na}$  could contribute to the action potential's rate of decline. The axon's cable properties (e.g. resistance or capacitance) could also vary among species. Previous work has demonstrated that, within a species, seasonal changes in the giant axon's internal resistance can influence conduction velocity (Rosenthal and Bezanilla, 2000b).

Do these data describe temperature adaptations? To answer this question, several factors should first be considered. Does

the giant axon system mediate an equivalent function in all the species tested? On the basis of similarities in anatomy and behavior, it is assumed that for each species the giant axon system regulates the jet-propelled escape response (Otis and Gilly, 1990; Young, 1938) and plays a role in feeding behavior (Preuss and Gilly, 2000). Are these species sufficiently close on a phylogenetic level to permit a meaningful comparison? Although there are no established standards, all four species are members of the family Loliginidae. On the basis of recent phylogenetic studies using mitochondrial DNA sequences, the three *Loligo* species are more closely related to each other than to other members of the genus. The species *S. sepioidea* is the outlier (Anderson, 2000). Therefore, when considering our data, more weight should be given to physiological differences that varied within the genus *Loligo* (e.g. the level of  $g_K$ ). All three species of *Loligo* are active pelagic predators. Although *S. sepioidea* are more domercile, it is probable that the giant axon system mediates the same basic function for all the squid species tested.

It is also important to consider why a physiological difference would be adaptive. First, the action potential's duration will be considered in terms of simple rate compensation. Is it necessary for species that inhabit different thermal environments to maintain a similar action potential duration at their native temperatures? If so, modifications of the underlying ionic conductances are required. Data from this study only partially support this view. Action potentials from

*L. opalescens* giant axons are relatively fast and those from *S. sepioidea* are slow. However, the rate compensation is not complete. On average, there is an approximately 5 °C shift in the fall times between *L. opalescens* and *S. sepioidea* and an overall shift of approximately 7.5 °C in the total action potential duration (fall time plus rise time). The temperature difference between these two species' environment is approximately double this. Clearly, there is not perfect rate compensation. When considering the purpose of the giant axon's action potential, to stimulate an escape jet, the necessity to compensate the duration in the first place is not immediately apparent. A single action potential in the giant axon produces an all-or-none contraction of the mantle musculature (Prosser and Young, 1937; Young, 1938). Does the duration of this action potential matter? A better understanding of the relationship between temperature, action potential duration and mantle contraction could help shed light on this issue.

An alternative hypothesis is that the action potential broadening, seen in the species from warmer habitats (*L. plei* and *S. sepioidea*), is merely a consequence of an adaptation to avoid action potential failure at high temperatures. As discussed in the Results section, action potentials in the two species from colder habitats fail at approximately 29 °C. The temperature range for both *L. plei* and *S. sepioidea* can approach this level. In fact, in our hands, both species survive in tanks maintained at this temperature. Using the Hodgkin and Huxley paradigm, decreases in  $g_K$  lead to increases in the failure temperature because less  $g_K$  competes with  $g_{Na}$  following stimulation. Action potentials from both 'warm' species exhibited a reduced  $g_K$  and elevated failure temperature. Other factors, however, could also contribute to differences in failure temperature (e.g. differences in  $Na^+$  channel inactivation). Clearly, avoiding action potential failure would be an adaptational advantage.

The reported changes in normalized conduction velocity can also be viewed in terms of compensatory adaptations. The conduction velocity of the giant axon of *S. sepioidea*, at all temperatures, is slower than that of *Loligo* species. In fact, the shift of approximately 10 °C between the conduction velocity *versus* temperature relationships is in reasonable agreement with the temperature ranges for these two species. Thus, to make the escape response as fast as possible, *Loligo* species have more  $g_{Na}$  in their axons to compensate for a relatively cold environment. It is important to note, however, that there is no apparent rate compensation within the genus *Loligo*, even though the species utilized in this study span a considerable range of habitat temperature. A previous study, using two *Loligo* species, hypothesized that a change in the slope of the conduction velocity *versus* temperature relationship was a temperature adaptation (Easton and Swenberg, 1975). In our study, at temperatures above 7 °C, there is no evidence for a change in the slope of the conduction velocity *versus* temperature relationship. Members of the genus *Loligo* are not commonly found below this temperature.

At present, we consider the physiological properties identified in this study as reasonable candidates for temperature

adaptations. Similar investigations utilizing more representatives within the family Loliginidae would help clarify the issue. These findings are interesting in light of the considerable attention that has been paid to the theory of homeoviscous adaptation (Macdonald, 1988; Sinensky, 1974). No comparative data exist for membrane lipid viscosity in the giant axon; however, homeoviscous adaptation would be expected to affect the rates of ion channel gating. These data suggest that absolute conductance levels are more likely to be targets of adaptation. However,  $Na^+$  channel inactivation and deactivation kinetics need to be measured. For these and other studies, the squid giant axon remains an excellent system in which to study temperature adaptation in nerve.

These investigations benefited from the kind efforts and aid of a great number of people. In Caracas, Venezuela, we wish to thank Drs R. DiPolo, C. Caputo and G. Whittetbury, H. Rojas and the rest of the IVIC staff. In Mochima, Venezuela, we thank R. Penot, Jesus Fuentes and Antonio Cariaco, expert procurers of 'chopos' and 'chipirones', at the Fundaciencia Marine Laboratory. At the Marine Biological Laboratory in Woods Hole, we thank Drs D. Gadsby, P. DeWeer, R. Rakowski, M. Holmgren and R. Hanlon. Finally, we thank John's Sportfishing in Marina Del Rey for kindly providing specimens of *L. opalescens*. This work was supported by GM20314 and GM30376 and a travel award from the UCLA Latin America Studies Program.

## References

- Adrian, R. H. (1975). Conduction velocity and gating current in the squid giant axon. *Proc. R. Soc. Lond. B* **189**, 81–86.
- Anderson, F. E. (2000). Phylogeny and historical biogeography of the loliginid squids (Mollusca: Cephalopoda) based on mitochondrial DNA sequence data. *Mol. Phylog. Evol.* **15**, 191–214.
- Armstrong, C. M. and Bezanilla, F. (1977). Inactivation of the sodium channel. II. Gating current experiments. *J. Gen. Physiol.* **70**, 567–590.
- Armstrong, C. M., Bezanilla, F. and Rojas, E. (1973). Destruction of sodium conductance inactivation in squid axons perfused with pronase. *J. Gen. Physiol.* **62**, 375–391.
- Armstrong, C. M. and Hille, B. (1998). Voltage-gated ion channels and electrical excitability [see comments]. *Neuron* **20**, 371–380.
- Bezanilla, F. (2000). The voltage sensor in voltage-dependent ion channels. *Physiol. Rev.* **80**, 555–592.
- Bezanilla, F. and Armstrong, C. M. (1977). Inactivation of the sodium channel. I. Sodium current experiments. *J. Gen. Physiol.* **70**, 549–566.
- Bezanilla, F., Rojas, E. and Taylor, R. E. (1970). Sodium and potassium conductance changes during a membrane action potential. *J. Physiol., Lond.* **211**, 729–751.
- Bezanilla, F., Taylor, R. E. and Fernández, J. M. (1982a). Distribution and kinetics of membrane dielectric polarization. I. Long-term inactivation of gating currents. *J. Gen. Physiol.* **79**, 21–40.
- Bezanilla, F., Vergara, J. and Taylor, R. E. (1982b). Voltage clamping of excitable membranes. *Meth. Exp. Physiol.* **20**, 445–511.
- Boyle, P. R. (1983). *Cephalopod Life Cycles*. London: Academic Press.
- Chapman, R. A. (1967). Dependence on temperature of the conduction velocity of the action potential of the squid giant axon. *Nature* **213**, 1143–1144.
- Chatfield, P. O., Lyman, C. P. and Irving, L. (1953). Physiological adaptation to cold of peripheral nerve in the leg of the herring gull (*Larus argentatus*). *Am. J. Physiol.* **172**, 639–644.
- Chen, Y., Sun, X. D. and Herness, S. (1996). Characteristics of action potentials and their underlying outward currents in rat taste receptor cells. *J. Neurophysiol.* **75**, 820–831.

- Easton, D. M. and Swenberg, C. E.** (1975). Temperature and impulse velocity in giant axon of squid *Loligo pealei*. *Am. J. Physiol.* **229**, 1249–1253.
- Hixon, R. F., Hanlon, R. T., Gillespie, S. M. and Griffin, W. L.** (1980). Squid fishery in Texas: biological, economic and market considerations. *Mar. Fish. Rev.* **42**, 44–50.
- Hodgkin, A.** (1975). The optimum density of sodium channels in an unmyelinated nerve. *Phil. Trans. R. Soc. Lond. B* **270**, 297–300.
- Hodgkin, A. L. and Huxley, A. F.** (1952). A quantitative description of membrane current and its application to conduction and excitation in nerve. *J. Physiol., Lond.* **117**, 500–541.
- Hodgkin, A. L. and Katz, B.** (1949). The effect of temperature on the electrical activity of the giant axon of the squid. *J. Physiol., Lond.* **109**, 240–249.
- Huxley, A. F.** (1959). Ion movements during nerve activity. *Ann. N.Y. Acad. Sci.* **81**, 221–246.
- Kaab, S., Nuss, H. B., Chiamvimonvat, N., O'Rourke, B., Pak, P. H., Kass, D. A., Marban, E. and Tomaselli, G. F.** (1996). Ionic mechanism of action potential prolongation in ventricular myocytes from dogs with pacing-induced heart failure. *Circ. Res.* **78**, 262–273.
- Lagerspetz, K. Y. and Talo, A.** (1967). Temperature acclimation of the functional parameters of the giant nerve fibres in *Lumbricus terrestris*. I. Conduction velocity and the duration of the rising and falling phase of the action potential. *J. Exp. Biol.* **47**, 471–480.
- Liu, T. I., Lebaric, Z. N., Rosenthal, J. J. C. and Gilly, W. F.** (2001). Natural substitutions at highly conserved T1-domain residues perturb processing and functional expression of squid Kv1 channels. *J. Neurophysiol.* **85**, 61–71.
- Macdonald, A. G.** (1988). Application of the theory of homeoviscous adaptation to excitable membranes: pre-synaptic processes. *Biochem. J.* **256**, 313–327.
- Macdonald, J. A.** (1981). Temperature compensation in the peripheral nervous system: Antarctic vs. temperate poikilotherms. *J. Comp. Physiol. A* **142**, 411–418.
- MacDonald, J. A., Montgomery, J. C. and Wells, R. M. G.** (1988). The physiology of McMurdo Sound fishes: current New Zealand research. *Comp. Biochem. Physiol.* **90B**, 567–578.
- Neumeister, H., Ripley, B., Preuss, T. and Gilly, W. F.** (2000). Effects of temperature on escape jetting in the squid *Loligo opalescens*. *J. Exp. Biol.* **203**, 547–557.
- Otis, T. S. and Gilly, W. F.** (1990). Jet-propelled escape in the squid *Loligo opalescens*: concerted control by giant and non-giant motor axon pathways. *Proc. Natl. Acad. Sci. USA* **87**, 2911–2915.
- Preuss, T. and Gilly, W. F.** (2000). Role of prey-capture experience in the development of the escape response in the squid *Loligo opalescens*: a physiological correlate in an identified neuron. *J. Exp. Biol.* **203**, 559–565.
- Prosser, C. L. and Nelson, D. O.** (1981). The role of nervous systems in temperature adaptation of poikilotherms. *Annu. Rev. Physiol.* **43**, 281–300.
- Prosser, C. L. and Young, J. Z.** (1937). Responses of muscles of the squid to repetitive stimulation of the giant nerve fibers. *Biol. Bull.* **73**, 237–241.
- Rojas, E., Bezanilla, F. and Taylor, R. E.** (1970). Demonstration of sodium and potassium conductance changes during a nerve action potential. *Nature* **225**, 747–748.
- Rosenthal, J. J. C. and Bezanilla, F.** (1998). Evidence for RNA editing in squid giant axon. *Am. Zool.* **37**, 190A.
- Rosenthal, J. J. C. and Bezanilla, F.** (2000a). Editing of delayed rectifier K<sup>+</sup> channel mRNA in squid giant axon. *Biophys. J.* **78**, 214A.
- Rosenthal, J. J. C. and Bezanilla, F.** (2000b). Seasonal variation in conduction velocity of action potentials in squid giant axons. *Biol. Bull.* **199**, 135–143.
- Rosenthal, J. J. and Gilly, W. F.** (1993). Amino acid sequence of a putative sodium channel expressed in the giant axon of the squid *Loligo opalescens*. *Proc. Natl. Acad. Sci. USA* **90**, 10026–10030.
- Rosenthal, J. J., Vickery, R. G. and Gilly, W. F.** (1996). Molecular identification of SqKv1A. A candidate for the delayed rectifier K channel in squid giant axon. *J. Gen. Physiol.* **108**, 207–219.
- Sinensky, M.** (1974). Homeoviscous adaptation – a homeostatic process that regulates the viscosity of membrane lipids in *Escherichia coli*. *Proc. Natl. Acad. Sci. USA* **71**, 522–525.
- Summers, W. C.** (1969). Winter population of *L. pealei* in the mid-Atlantic Bight. *Biol. Bull.* **137**, 202–216.
- Taylor, R. E.** (1963). Cable theory. In *Physical Techniques in Biological Research*, vol. 6 (ed. W. L. Nastuk), pp. 219–262. New York: Academic Press.
- Thüringer, D., Deroubaix, E., Coulombe, A., Coraboeuf, E. and Mercadier, J. J.** (1996). Ionic basis of the action potential prolongation in ventricular myocytes from Syrian hamsters with dilated cardiomyopathy. *Cardiovasc. Res.* **31**, 747–757.
- Vandenberg, C. A. and Bezanilla, F.** (1991). A sodium channel gating model based on single channel, macroscopic ionic and gating currents in the squid giant axon. *Biophys. J.* **60**, 1511–1533.
- Voss, G. L.** (1956). A review of the cephalopods of the Gulf of Mexico. *Bull. Mar. Sci. Gulf Caribb.* **6**, 85–119.
- Weight, F. F. and Erulkar, S. D.** (1976). Synaptic transmission and effects of temperature at the squid giant synapse. *Nature* **261**, 720–722.
- Whitaker, J. D.** (1978). A contribution to the biology of *Loligo pealei* and *Loligo plei* (Cephalopoda, Myopsida) off the southeastern coast of the United States. MS thesis, pp. 186. College of Charleston.
- Whitaker, J. D.** (1980). Squid catches resulting from trawl surveys of the southeastern United States. *Mar. Fish. Rev.* **42**, 39–43.
- Young, J. Z.** (1938). The functioning of the giant nerve fibres of the squid. *J. Exp. Biol.* **15**, 170–185.
- Zhang, L. and McBain, C. J.** (1995). Potassium conductances underlying repolarization and after-hyperpolarization in rat CA1 hippocampal interneurons. *J. Physiol., Lond.* **488**, 661–672.